ARTICLE
Journal of Cellular Biochemistry 115:996–1005 (2014)

Journal of Cellular Biochemistry

Sirt1 Activation Ameliorates Renal Fibrosis by Inhibiting the TGF-β/Smad3 Pathway

Xin-Zhong Huang,[1,2] Donghai Wen,[1] Min Zhang,[1] Qionghong Xie,[1] Leting Ma,[1] Yi Guan,[1] Yueheng Ren,[1] Jing Chen,[1] and Chuan-Ming Hao[1]*

[1]*Division of Nephrology, Huashan Hospital, Fudan University, Shanghai 200040, China*
[2]*Division of Nephrology, Affiliated Hospital of Nantong University, Nantong 226001, China*

ABSTRACT

TGF-β signaling plays an important role in the pathogenesis and progression of chronic kidney disease (CKD). Smad3, a transcription factor, is a critical fibrogenic mediator of TGF-β. Sirt1 is a NAD^+-dependent deacetylase that has been reported to modify a number of transcription factors to exert certain beneficial health effects. This study examined the effect of Sirt1 on Smad3 and its role in CKD. Resveratrol attenuated the expression of extracelluar matrix proteins in both the remnant kidney of 5/6th nephrectomized rats and cultured mesangial cells (MMCs) exposed to TGF-β1. The effect of resveratrol was substantially attenuated in cultured MMCs for which Sirt1 had been knocked down by an shRNA lentivirus. Overexpression of Sirt1 attenuated TGF-β1-induced extracelluar matrix expression in cultured cells. Co-immunoprecipitation studies suggested that Sirt1 could bind with Smad3. Resveratrol treatment enhanced this binding and reduced acetylation levels of Smad3. Resveratrol inhibited the transcription activity of Smad3. Knockdown of Sirt1 increased acetylated Smad3 and substantially enhanced the transcriptional activity following TGF-β1. Finally, Sirt1 deficiency aggravated renal function damage and markedly enhanced fibrosis in the remnant kidney of 5/6 nephrectomized mice. Taken together, these results identify Sirt1 as an important protective factor for renal fibrosis in a CKD rodent model, and the protective function of Sirt1 is attributable to its action on TGF-β/Smad3 signaling. Therefore, we suggest that Sirt1 may be a potential therapeutic target for the treatment of CKD. J. Cell. Biochem. 115: 996–1005, 2014. © 2013 Wiley Periodicals, Inc.

KEY WORDS: Sirt1; CHRONIC KIDNEY DISEASE; FIBROSIS; RESVERATROL

It is well-documented that fibrosis plays an important role in the pathogenesis and progression of chronic kidney disease (CKD). Accumulating evidence [Border and Noble, 1997; Schnaper et al., 2002; Wang et al., 2005] indicates a central role for TGF-β and its downstream signaling cascades in activating cellular pathomechanisms that underlie the progression of renal diseases. TGF-β has been shown to be a critical regulator of cell proliferation, differentiation, apoptosis, immune response, and extracellular matrix (ECM) production [Bottinger and Bitzer, 2002; Schnaper et al., 2002; Liu, 2006]. The signaling mechanism by which TGF-β induces ECM production has been documented. TGF-β signals through the heteromeric complex of TGF-β type I receptor with TGF-β type II receptor to activate Smad2 and Smad3 phosphorylation at their C termini and assemble into stable heteromeric complexes with Smad4 [Roberts et al., 2003; Flanders, 2004]. These complexes are the functional entities that translocate into the nucleus, where they can interact with various transcription factors and regulate the expression of TGF-β target genes [Shi and Massague, 2003; Roberts et al., 2006]. Recently, Smad3 has also been shown to be acetylated at the Lys-378 by the p300/CBP in a TGF-β-dependent manner, regulating the DNA binding and transcriptional activity of Smad3 [Simonsson et al., 2006; Inoue et al., 2007; Li et al., 2010].

Sirt1 belongs to a highly conserved family of NAD^+-dependent deacetylase and has been reported to deacetylate the lysine residues of a number of nuclear proteins, such as p53 [Yuan et al., 2011], NF-kB [Salminen and Kaarniranta, 2009], PGC-1a [Amat et al., 2009], CBP/p300 [Das et al., 2009], and forkhead family proteins [Brunet

Xinzhong Huang and Donghai Wen contributed equally to this work.
Disclosures: The authors declare no conflict of interest.

Grant sponsor: National Natural Science Fundation; Grant number: 81130075; Grant sponsor: Major State Basic Research Development Program of China (973 program); Grant number: 2012CB517700; Grant sponsor: 985 Project of China; Grant number: 985III-YFX0302; Grant sponsor: Science and Technology Foundation of Nantong; Grant number: BK2013006.

*Correspondence to: Prof. Chuan-Ming Hao, Division of Nephrology, Huashan Hospital, Fudan University, Shanghai, 200040, China. E-mail: chuanminghao@fudan.edu.cn

Manuscript Received: 6 October 2013; Manuscript Accepted: 6 December 2013
Accepted manuscript online in Wiley Online Library (wileyonlinelibrary.com): 19 December 2013
DOI 10.1002/jcb.24748 • © 2013 Wiley Periodicals, Inc.

et al., 2004]. Sirt1 is widely expressed throughout almost all mammalian organs, regulating stress resistance, DNA repair, and longevity [Hao and Haase, 2010]. A recent study demonstrated that Sirt1 could interact with TGF-β signaling and reduce apoptosis in TGF-β-treated measangial cells [Kume et al., 2007]. In addition, Sirt1 activation attenuates renal fibrosis in a unilateral ureteral obstruction model [He et al., 2010].

Resveratrol (RSV) is a polyphenol with antifibrotic and anti-inflammatory properties, which can be available in grape skins and in wines [Aubin et al., 2008; Hashem et al., 2008; Inanaga et al., 2009]. It has also been shown to activate Sirt1 which has health beneficial effect, including metabolic diseases [Park et al., 2012], neurological disorders [Rasouri et al., 2007], cardiac hypertrophy [Planavila et al., 2011], and aging [Queen and Tollefsbol, 2010].

The aim of the present study is to examine whether Sirt1 activation ameliorates TGF-β signaling through deacetylation of Smad3 and attenuates renal fibrosis in vivo in a chronic renal failure model and in vitro in murine mesangial cells (MMCs). The present study provides important experimental evidence supporting Sirt1 as a potential therapeutic target for CKD.

MATERIALS AND METHODS

ANIMAL MODELS

All animal studies were approved by the Institutional Animal Care and Use Committees of Fudan University. Rats and mice were maintained in the animal facility of Fudan University Medical Animal Center, where they were housed in a constant-temperature room with a 12-h dark/12-h light circle and allowed free access to standard rodent chow and water. Sprague-Dawley rats and wild-type C57BL/6J mice at 8 weeks of age were obtained from Fudan University Medical Animal Center. Male Sprague-Dawley rats weighing 200 to 220 g (8 weeks old) were anesthetized with 350 mg/kg body weight chloral hydrate via intraperitoneal injection. Forty rats underwent a 5/6-nephrectomy in which two thirds of the right kidney was first removed followed by the ablation of the left kidney 1 week later [Badid et al., 2000]. Sham-operated rats (Sham, $n = 10$) underwent the same procedure without surgical reduction of the kidney. Forty rats with 5/6Nx were later administered either RSV (20 mg/kg, Copalyton Chemical Materials Co., Ltd, Shanghai, China) (Nx + RSV, $n = 20$) or vehicle (Nx, $n = 20$) via daily oral gavage starting 1 week after surgery and continuing for a period of 12 weeks. Vehicle-treated groups received an equal volume of normal saline. At 4-week intervals, daily urinary protein excretion was determined by the biuret method after urine collection from rats individually housed in metabolic cages for 24 h. At the end of the study, the rats were anesthetized, their blood was collected by cardiac puncture, and their kidney tissue samples were collected for immunohistochemistry, Western blot, and real-time PCR as described previously [Zhang et al., 2011].

GENERATION OF SIRT1 CONDITIONAL KO MICE

Mice with 1 allele of Sirt1 gene deletion were obtained by crossing a $Sirt1^{fl/+}$ mouse (C57BL/6 J) with a universal Cre mouse (C57BL/6 J). This mouse was further bred with a C57BL/6J mouse to generate heterozygous Sirt1-knockout mice ($Sirt1^{+/-}$) and their wild-type littermates ($Sirt1^{+/+}$). The generation and characterization of the Sirt1 flox mouse and the universal Cre transgenic mouse were described previously [Cheng et al., 2003; He et al., 2010]. Male mice between 8 and 10 weeks of age were used in the present study. Under anesthesia (chloral hydrate), $Sirt1^{+/+}$ and $Sirt1^{+/-}$ mice were subjected to 5/6Nx (surgical resection of the lower and upper thirds of the left kidney with right Nx) (Nx, $n = 12$). Sham-operated $Sirt1^{+/+}$ and $Sirt1^{+/-}$ mice (Sham, $n = 8$) underwent the same procedure without surgical reduction of the kidney. At 4-week intervals, daily urinary protein excretion was determined by biuret method after urine collection from mice individually housed in metabolic cages for 24 h. Mice were sacrificed at 12 weeks after the operation. At the end of the study, the mice were anesthetized, their blood was collected by cardiac puncture, and their kidney tissue samples were collected for Western blot and real-time PCR.

CELL CULTURE

SV40-transformed murine mesangial cell (MMC) line cells (MES-13 cells) were purchased from the American Type Culture Collection (Manassas, VA) and cultured at 37°C in a 5% CO_2 atmosphere in Dulbecco's modified Eagle's medium (GIBCO) supplemented with 10% fetal calf serum, penicillin (100 U/ml), streptomycin (100 μg/ml), L-glutamine (2 mM), and glucose (100 mg/dl). A recombinant human TGF-β1 (R&D Systems, Minneapolis, MN) at concentrations of 2 ng/ml was added to the cell culture for periods of 0, 6, 12, and 24 h with or without RSV for detection of TGF-β/Smad3 signaling and fibrosis response. In addition, TGF-β1 at dosages of 1.0, 2.0, and 5.0 ng/ml was applied for 48 h for a dosage-dependent assay. At least three independent experiments were performed throughout the study.

DETERMINATION OF RENAL FUNCTION

Rats' serum creatinine and blood urea nitrogen levels were measured using an automated analyzer according to the manufacturer's instructions. Mice blood urea nitrogen was measured using Infinity™ Urea (Nitrogen) Liquid Stable Reagent (Thermo Fisher Scientific, Inc.) according to the manufacturer's instructions.

HISTOLOGICAL EXAMINATION

Tissues fixed in 4% paraformaldehyde/PBS were embedded in paraffin using routine protocols. Paraffin-embedded materials were sectioned at 4 μm for routine staining with PAS and Masson trichrome. Glomerulosclerosis was assessed in 50 glomeruli on PAS-stained sections under ×400 magnification using a semi-quantitative score from 0 to 4 (0, no sclerosis; 1, sclerosis up to 25% of glomeruli; 2, sclerosis from 25% to 50% of glomeruli; 3, sclerosis from 50% to 75% of glomeruli; 4, sclerosis >75% of glomeruli), and the results were averaged. For evaluating tubulointerstitial damage, 15 fields for each section (Masson trichrome stain) were evaluated at ×200 magnification using Image-Pro Plus 6.0 processing software (Media Cybernetics). The extent of tubulointerstitial damage was evaluated by counting the percentage of areas with tubular dilation, interstitial infiltration, and fibrosis per field of cortex. Scores from 0 to 4 were used (0, normal interstitium; 1, <25% of areas injured; 2, 26% to 50% of areas injured; 3, 51% to 75% of areas injured; 4, >75% of areas injured), and the results were averaged. All histological analyses were performed by two

investigators without knowledge of the origin of the slides, and the mean values were calculated.

SIRT1 KNOCKDOWN BY LENTIVIRUS CARRYING SIRT1-SELECTIVE SHRNA

Lentivirus infection was performed as previously described [He et al., 2010]. HEK293T cells were cotransfected with lentiviral pLKO.1 plasmid-carrying scrambled shRNA or Sirt1-selective shRNA, psPAX2 packaging plasmid, and pMD2.G envelope plasmid using Lipofectamine reagent. Twelve hours later, the medium containing the transfection reagent was removed and replaced with fresh complete DMEM plus 10% FBS and penicillin/streptomycin. Twenty-four hours later, the culture medium containing lentiviral particles was harvested from HEK293T cells and transferred to a polypropylene storage tube. Virus was stored in aliquots at –80°C. MMCs were later infected with appropriate amounts of lentiviral particles containing medium. Twenty-four hours later, virus-containing medium was removed and replaced with fresh medium. Infected MMCs were cultured for 3 days, and Western blotting was subsequently performed to examine the efficiency of protein knockdown.

SIRT1 OVEREXPRESSION

To force overexpression of Sirt1 in MMCs, a pCruzHA-Sirt1 plasmid or control pCruzHA-empty vector were transfected into MMC using Lipofectamine 2000 (Invitrogen) as previously described. Characterization of Sirt1-overexpressing MMC was determined by Western blot with anti-Sirt1 antibody (Sigma–Aldrich mouse monoclonal, 1:500). After 48 h, cells were treated with or without TGF-β1 for 24 h. The levels of fibronectin and collagen I expression were determined by Western blot analysis.

REAL-TIME PCR

Total RNA was extracted from renal tissues or cultured MMCs using TRIzol® reagent (Invitrogen). Reverse transcription was performed using a first strand cDNA reverse transcription kit (Fermentas Life Sciences). Real-time PCR was performed using a SYBR Green/ROX qPCR Master Mix kit according to the manufacturer's instructions (Fermentas Life Sciences). The primers used were as follows: rat fibronectin forward 5′-TCGCTTTGACTTCACCACCAG and reverse 5′-CCTCGCTCAGTTCG-TACTCCAC; collagen I forward 5′-ATCCTGCCTATGTCGCTAT and reverse 5′-CCACAAGCGTGCTGTAGGT; β-actin forward 5′-GAGG-GAAATCGTGCGTGAC and reverse 5′-CTGGAAGGTGGACAGTGAG; mouse fibronectin forward 5′-CCAGGTTGATGATACTTCCATTGTT and reverse 5′-GCTCTGTGCTACTGCCTTCTACTG; collagen I forward 5′-ATCCTGCCTATGTCGCTAT and reverse 5′-CCACAAGCGTGCTG-TAGGT; Sirt1 forward 5′-GCAACAGCATCTTGCCTGAT and reverse 5′-GTGCTACTGGTCTCACTT; and β-actin forward 5′-CTGTCCCTG-TATGCCTCTG and reverse 5′-ATGTCACGCACGATTTCC. The ratio for the mRNA of interest was normalized with β-actin and expressed as the mean ± SE

IMMUNOPRECIPITATION

Immunoprecipitation analysis was performed as described previously [Chen et al., 2005]. Kidney tissues and cultured cells were homogenized and lysed on ice for 15 min in hypotonic lysis buffer (10 mM HEPES, pH 7.9, 1 mM EDTA, 15 mM KCl, 2 mM $MgCl_2$, 1 mM Dithiothreitol, and 0.8% Nonidet P-40) containing protease inhibitor mixture (Roche Applied Science). The cell lysates were centrifuged at 4°C at 3,000*g* for 10 min. The pellets were resuspended in high salt buffer (hypotonic buffer with 420 mM NaCl and 25% glycerol), rotated for 30 min at 4°C, and centrifuged at 13,000*g* for 30 min. The supernatants were used as nuclear extracts. Immunoprecipitations were carried out by adding the appropriate antibodies plus protein A/G-Agarose beads followed by incubation at 4°C for 4 h. Nonspecific IgG (Santa Cruz Biotechnology) was used as control. The immunoprecipitates were washed extensively in IP buffer (Tris 20 mM, pH 7.5, NaCl 150 mM, EDTA 1 mM, EGTA, 1 mM, Triton-100 1%) and were resuspended in 30 μl of 2× sample buffer. The samples were boiled for 2 min, and 20 μl of precipitated proteins were added to each lane of an SDS-PAGE gel.

WESTERN BLOTTING

Protein from kidney tissues and cultured cells was extracted with RIPA lysis buffer, and Western blot analysis was performed as described previously [Chen et al., 2006]. After blocking nonspecific binding with 5% Carnation nonfat dry milk for 1 h at room temperature, membranes were later incubated with primary antibody overnight at 4°C. The primary antibodies used were anti-Sirt1 antibody (Millipore rabbit polyclonal, 1:1,000; Sigma–Aldrich mouse monoclonal, 1:500), anti-collagen I antibody (Abcam rabbit polyclonal, 1:500), anti-fibronectin antibody (Sigma–Aldrich chicken polyclonal, 1:500), anti-Smad3 antibody (Cell Signaling Technology rabbit polyclonal, 1:1,000), anti-Phospho-Smad3 antibody (Ser423/425) (Cell Signaling Technology rabbit monoclonal, 1:1,000), anti-Acetylated-Lysine antibody (Ac-K-103) (Cell Signaling Technology mouse monoclonal, 1:1,000)and anti-β-actin antibody (Sigma–Aldrich mouse monoclonal, 1:2,000). After three washes, the membrane was incubated with horseradish peroxidase–conjugated secondary antibody (Jackson Immuno Research Laboratories, 1:5,000) for 1 h at room temperature followed by three washes with TBST. Antibody labeling was visualized by the addition of chemiluminescence reagent (Amersham Biosciences), and the membrane was exposed to Kodak XAR-5 film.

SMAD3-DEPENDENT PROMOTER ASSAY

MMC was transiently transfected with the Smad3/4-responsive promoter p(CAGA)12-Luc and the internal control pRL-TK vector (Promega) as described previously [Dennler et al., 1998; Meng et al., 2010] with or without lentivirus carrying Sirt1-selective shRNA. The transfection procedure was performed using Lipofectamine 2000 (Invitrogen) according to the manufacturer's instructions. After transfection and serum starving for 24 h, TGF-β1 (2 ng/ml) and RSV (25 μM) were added to the cells for 24 h. A Dual Luciferase assay kit (Promega) was used to measure both Firefly and Renilla luciferase activity in the transfected MMC. Relative luciferase activity was defined as Smad3 reporter Firefly luciferase activity adjusted by Renilla luciferase activity expressed from pRL-TK. Data are presented as fold induction compared with control group. Three independent experiments were performed throughout the study.

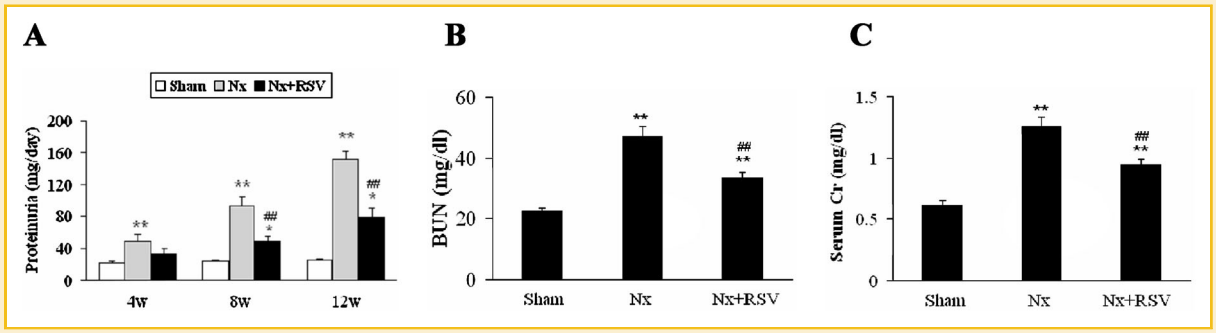

Fig. 1. RSV preserves renal function in 5/6-nephrectomized rats. Changes in (A) proteinuria, (B) BUN, and (C) serum creatinine of sham-operated rats (Sham) and 5/6-nephrectomized rats treated with vehicle (Nx) or RSV (Nx + RSV) are shown. Data are means ± SE, $^{*}P < 0.05$, $^{**}P < 0.01$ versus Sham; $^{\#}P < 0.05$, $^{\#\#}P < 0.01$ versus Nx.

STATISTICAL ANALYSIS

All data examined are expressed as means ± SEM. Statistical analyses of the data were performed using SPSS version 12.0 Software (IBM). Comparisons between groups were made using one-way ANOVA or Student's *t*-test. $P < 0.05$ was considered to be statistically significant.

RESULTS

RSV ATTENUATES KIDNEY DAMAGE IN 5/6NX RATS

Figure 1 presents the renal function including blood urea nitrogen and serum creatinine, and proteinuria of 5/6Nx rats treated with or without RSV. 5/6Nx significantly increased urinary protein excretion compared with a sham operation. RSV treatment significantly blunted the increase of urinary protein excretion in the 5/6Nx rats (Fig. 1A). BUN and serum creatinine levels were significantly increased following 5/6Nx at the 12th week. RSV treatment significantly reduced the increase in BUN and serum creatinine in 5/6Nx rats (Fig. 1B,C).

Figure 2 represents the periodic acid-Schiff (PAS) and Masson trichrome stainings of the kidneys. The kidneys of the 5/6Nx rats were characterized by glomerular sclerosis and tubulointerstitial fibrosis. Semi-quantitative analysis shows that the glomerular sclerosis index (1.56 ± 0.34 vs. 0.35 ± 0.08) and tubulointerstitial fibrosis (1.47 ± 0.29 vs. 0.18 ± 0.04) were significantly increased in 5/6Nx rats compared with sham rats ($P < 0.01$). RSV substantially reversed these changes (Fig. 2A,B).

Fibronectin and type I collagen expression in the kidney were higher in the 5/6Nx rats than sham rats, as assessed by real-time PCR

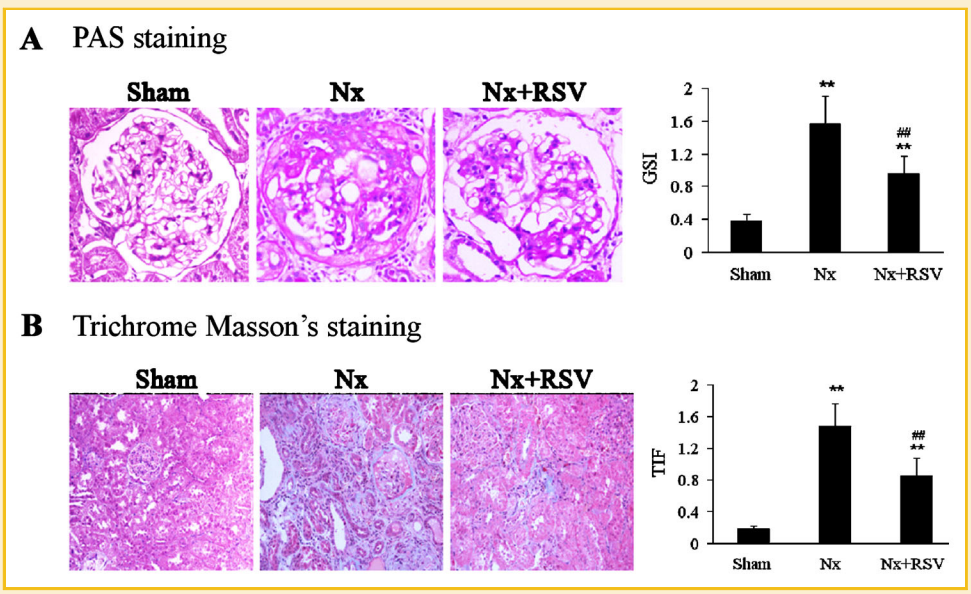

Fig. 2. Effects of RSV on renal histology in 5/6-nephrectomized rats. Light microscopic findings and quantitative analysis in the study groups. Representative pictures stained with (A) PAS and (B) Masson trichrome in sham-operated rats, 5/6Nx rats, and 5/6Nx + RSV rats. $^{**}P < 0.01$ versus Sham; $^{\#\#}P < 0.01$ versus 5/6Nx. Magnifications: ×400 in A; ×200 in B.

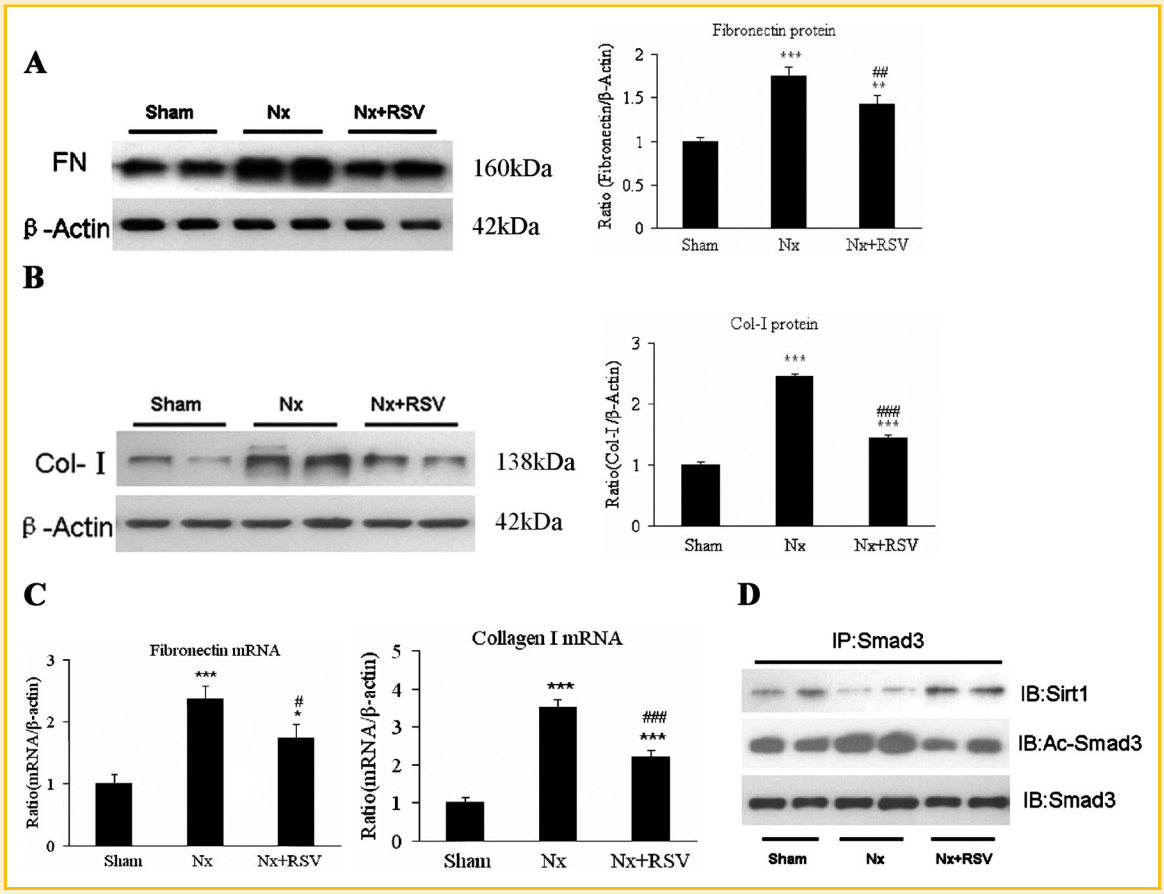

Fig. 3. Effects of RSV on renal fibrotic gene expression levels and Smad3 acetylation levels in the kidney of 5/6 nephrectomized rats. A: Fibronectin expression by Western blot. B: Type I collagen expression by Western blot. C: Fibronectin and type I collagen expression by real-time PCR. Data are means ± SE; The values were normalized to the β-actin values and then expressed as relative quantification. $^{*}P < 0.05$, $^{**}P < 0.01$, $^{***}P < 0.001$ versus Sham; $^{\#}P < 0.05$, $^{\#\#}P < 0.01$, $^{\#\#\#}P < 0.001$ versus Nx. D: Immunoprecipitation/Western blot of Sirt1 and Smad3 acetylation in each group.

and Western blot. RSV treatment significantly reduced fibronectin and type I collagen expression in these rats (Fig. 3A–C).

RSV REDUCES EXTRACELLULAR MATRIX PRODUCTION THROUGH SIRT1 IN CULTURED MESANGIAL CELLS

In cultured MMCs, TGF-β1 (2 ng/ml, 24 h) significantly increased fibronectin and collagen I expression (Fig. 4A,B and Fig. S1A, B). RSV dose-dependently down-regulated TGF-β1-induced fibronectin and collagen I expression in cultured cells (Fig. 4C and Fig. S1C).

To examine whether the effect of RSV on ECM protein production depends on Sirt1, Sirt1 was downregulated using a lentivirus carrying a Sirt1-selective shRNA in MMCs (Fig. 5A). Knocking down Sirt1 markedly attenuated the protective effect of RSV, supporting that Sirt1 mediates the effect of RSV (Fig. 5B).

To examine further the role of Sirt1 in ECM production, we overexpressed Sirt1 in MMCs. As shown in Figure 5C, Western blot shows that MMCs overexpressing Sirt1 significantly attenuated TGF-β1-induced extracelluar matrix expression at 24 h, resulting in a 53.2% and 43.6% decrease in fibronectin and collagen I expression, respectively, compared with the control group (Fig. 5D), supporting the protective effect of Sirt1 on renal fibrosis.

Sirt1 REDUCES SMAD3 ACETYLATION IN 5/6NX RATS AND IN CULTURED MMCS TREATED WITH TGF-β1

To assess the acetylation levels of Smad3, first, Smad3 was immunoprecipitated, and the acetyl group was determined by an anti-acetyl antibody. As shown in Figure 3D, the acetylated-Smad3 levels increased in the remnant kidney and were reduced in the rats treated with RSV. Further studies showed that Sirt1 was co-immunoprecipitated with Smad3. This binding of Sirt1 to Smad3 was reduced in the remnant kidney, which was associated with increased acetylation levels of Smad3. RSV increased the binding of Sirt1 and Smad3 and reduced acetylated Smad3. Smad3 phosphorylation levels were increased in the remnant kidney, as reported (Fig. S2A). RSV treatment did not alter the phosphorylated Smad3 in this model. These results suggest that the renal protective effect of RSV was independent of the phosphorylation of Smad3 but may be associated with Smad3 acetylation.

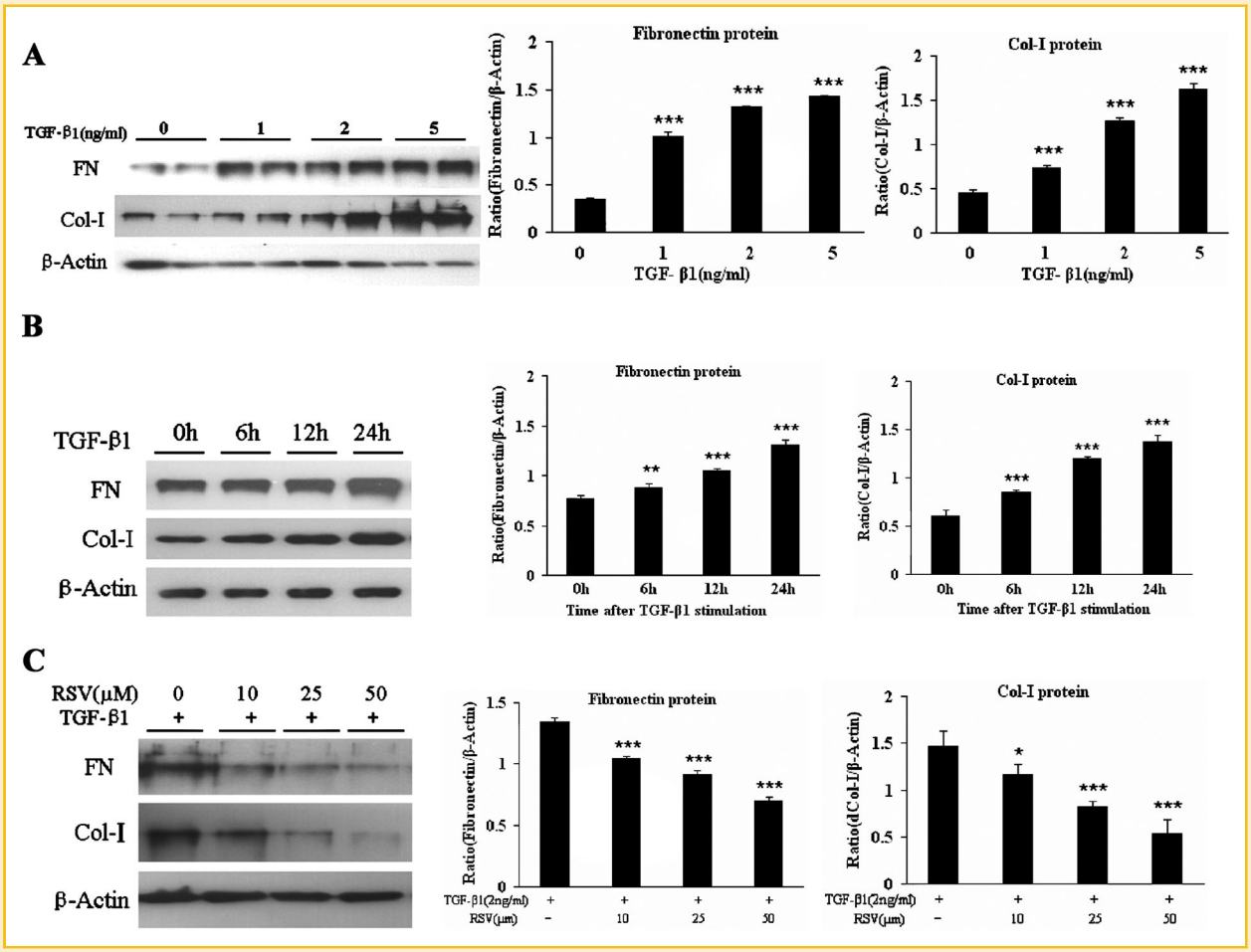

Fig. 4. Effect of RSV on TGF-β1-induced fibronectin and collagen I protein expression. A: Western blot analysis shows that TGF-β1 induces fibronectin and collagen I protein expression at 48 h in a dosage-dependent manner. B: Western blot analysis shows that TGF-β1 (2 ng/ml) induces fibronectin and collagen I protein expression in a time-dependent manner. C: Western blot analysis shows that RSV down-regulates TGF-β1 (2 ng/ml) induced fibronectin and collagen I protein expression at 24 h in a dosage-dependent manner. Data are means ± SE for three independent experiments. $^{*}P < 0.05$, $^{**}P < 0.01$, $^{***}P < 0.001$ versus dosage or time 0, or RSV 0.

In cultured MMCs, as shown in Figure 6A, TGF-β1 increased acetylation levels of Smad3, and RSV dosage-dependently reduced the acetylation of Smad3. Co-immunoprecipitation showed a binding of Smad3 with Sirt1. TGF-β1 reduced this binding and was associated with increased acetylation of Smad3. RSV treatment reversed this process. Knocking down Sirt1 increased TGF-β1-induced acetylation of Smad3 (Fig. 6B). Phospho-Smad3 levels were increased following TGF-β1 in MMCs, as expected (Fig. S2B). RSV treatment did not alter the phosphorylation of Smad3.

SIRT1 INHIBITED SMAD3 TRANSCRIPTION ACTIVITY

To examine the effect of Sirt1 activity and Smad3 acetylation on Smad3 transcriptional activity, a Smad3-responsive promoter assay was used. As shown in Figure 6C, knocking down Sirt1 substantially enhanced TGF-β1-induced Smad3-dependent promoter activity. RSV treatment significantly reduced TGF-β1-induced Smad3-dependent promoter activity. Knocking down Sirt1 significantly attenuated the effects of RSV.

SIRT1 DEFICIENCY ENHANCES RENAL DAMAGE IN 5/6 NEPHRECTOMIZED MICE

Finally, we examined the importance of Sirt1 in renal fibrosis in vivo using a mouse line deficient for Sirt1. Because homozygous Sirt1 knockout ($Sirt1^{-/-}$) mice exhibit severe developmental defects and early postnatal lethality [Cheng et al., 2003], heterozygous Sirt1 knockout ($Sirt1^{+/-}$) mice were used for the present study. Heterozygous Sirt1 knockout mice developed normally, and their kidneys were histologically normal (Fig. S3). Reduced Sirt1 expression in the kidney of the $Sirt1^{+/-}$ mice has been demonstrated at mRNA level by real-time PCR (Fig. 7A) and protein level by Western blot analysis (Fig. 7B).

As shown in Figure 8A–C, urinary protein excretion, serum creatinine (SCr) and BUN levels significantly increased in $Sirt1^{+/+}$ mice at 12 weeks after 5/6 nephrectomy. Loss of one allele of Sirt1 significantly enhanced renal damage following 5/6 nephrectomy, exhibiting higher urinary protein excretion, SCr, and BUN compared with Sirt1 intact mice. Western blot analysis also indicated that

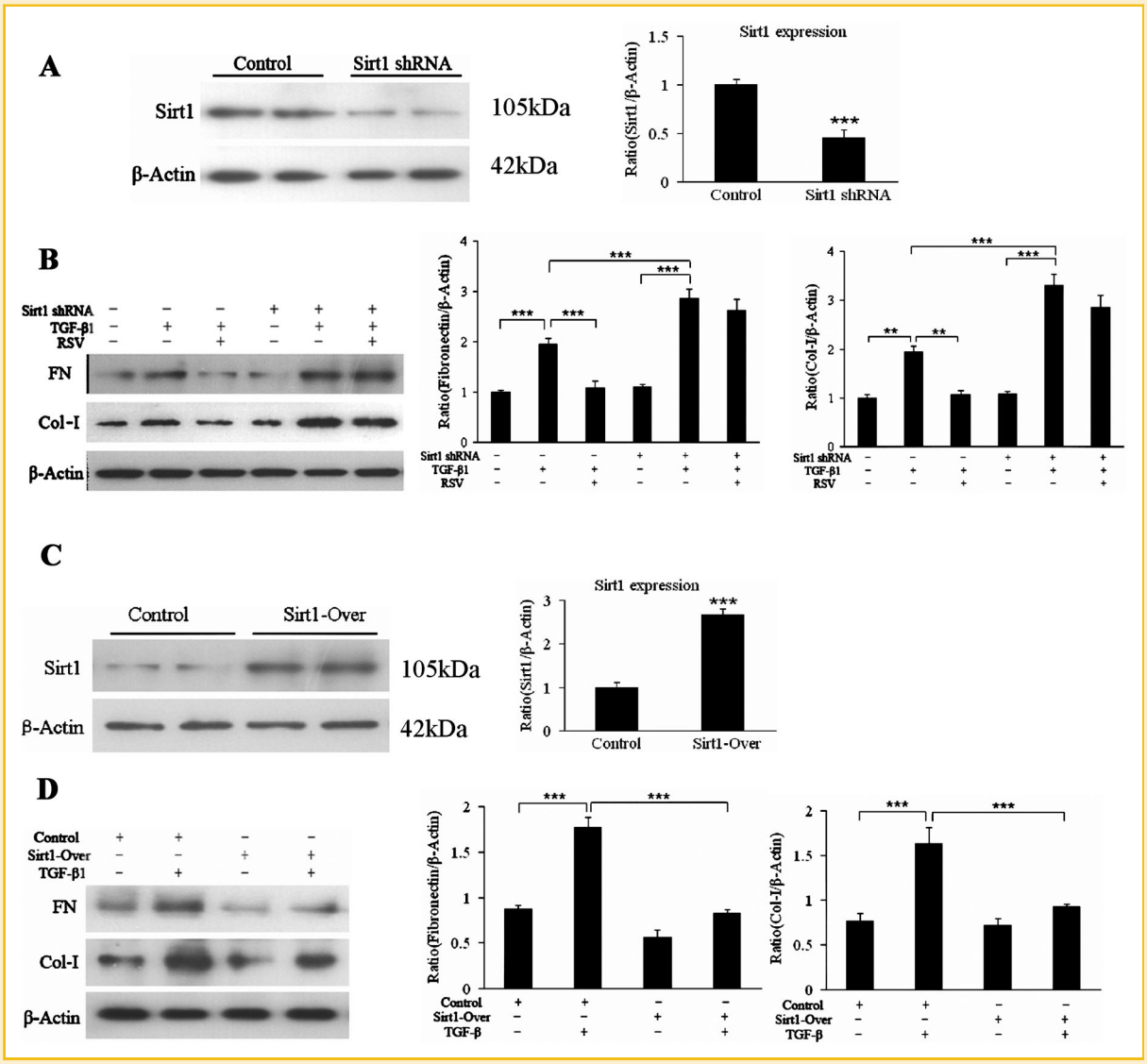

Fig. 5. Effects of Sirt1 knock-down or over-expression on fibronectin and collagen I protein expression induced by TGF-β1. A: MMCs were infected with lentivirus carrying Sirt1-selective shRNA or control virus. Expression of Sirt1 was examined by Western blot. $^{***}P < 0.001$ versus Control. B: Control or Sirt1 shRNAtreated MMCs were stimulated with TGF-β1 (2 ng/ml) and treated with or without Sirt1 activator RSV (25 μM) for 24 h. Expression of fibronectin and collagen was examined by Western blot. $^{**}P < 0.01$, $^{***}P < 0.001$ versus TGF-β1. C: MMCs were transfected with Sirt1 overexpression plasmid or control plasmid. Expression of Sirt1 was examined by Western blot. $^{***}P < 0.01$ versus Control. D: Control or Sirt1 overexpression plasmid-transfected MMCs were treated with or without TGF-β1 (2 ng/ml) for 24 h. Expression of fibronectin and collagen I was examined by Western blot. $^{***}P < 0.001$ versus Control + TGF-β1.

fibronectin and type I collagen expression in the 5/6Nx kidney of the $Sirt1^{+/-}$ mice was higher than in $Sirt1^{+/+}$ mice (Fig. 8D).

DISCUSSION

The present study demonstrates that RSV protects the remnant kidney of the 5/6 nephrectomized rat. RSV treatment significantly attenuates the decline of GFR in the 5/6 nephrectomized rats. In cultured MMCs, RSV reduces ECM protein expression induced by TGF-β1, and its effect depends on Sirt1. Sirt1 inhibits TGF-β1 signaling by deacetylating Smad3, and the loss of one allele of Sirt1 aggravates the kidney damage in 5/6 nephrectomized mice. These results suggest that renal Sirt1 is an antifibrotic factor and a potential therapeutic target for CKD.

The antifibrotic function of Sirt1 has been reported in heart failure [Tanno et al., 2010], cardiac fibrosis [Alcendor et al., 2007], hepatic steatosis [Costa Cdos et al., 2010], diabetic nephropathy [Kitada et al., 2011], and unilateral ureteral obstruction (UUO) [He et al., 2010]. This study provides strong evidence that Sirt1 can inhibit TGF-β1 signaling by deacetylating Smad3 and reducing kidney fibrosis, thereby protecting the kidney of a rodent model of CKD. We first found that RSV reduced urinary protein excretion and attenuated the decline of GFR in the 5/6 nephrectomized rats. To test whether the effect of RSV on the remnant kidney is associated with

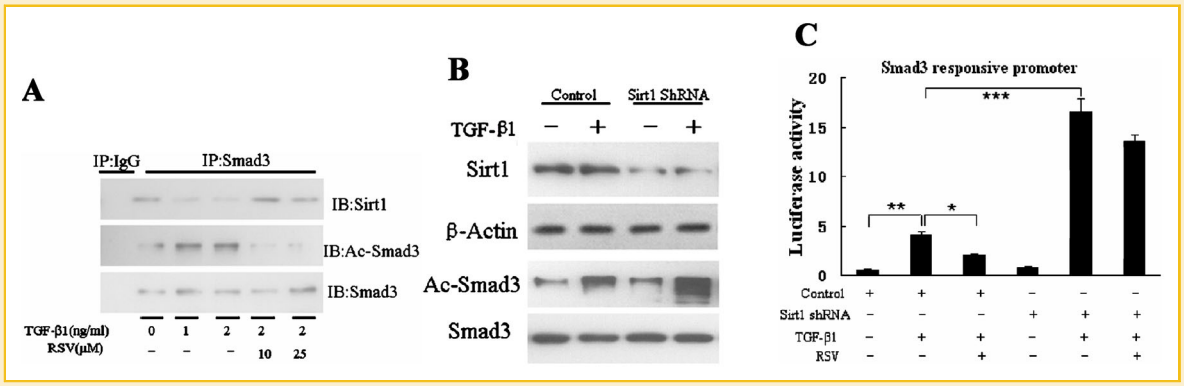

Fig. 6. Effect of RSV on TGF-β1-induced Smad3 acetylation levels in cultured measangial cells. A: Immunoprecipitation/Western blot of Sirt1 and Smad3 acetylation. B: Knocking down Sirt1 increased TGF-β1-induced the acetylation of Smad3. C: Smad3 promoter activity assay. $^{*}P < 0.05$, $^{**}P < 0.01$, $^{***}P < 0.001$ versus Control + TGF-β1.

Sirt1, we cultured renal MMCs. RSV treatment substantially reduced TGF-β1-induced ECM protein production. Knocking down Sirt1 not only enhanced TGF-β1's effect on ECM but also markedly blunted the protective effect of RSV. This finding supports that the effect of RSV is, at least partially, associated with its action on Sirt1. The protective effect of Sirt1 on CKD is further supported by a study using Sirt1-deficient mice. Loss of one allele of Sirt1 significantly aggravated the kidney damage following 5/6 nephrectomy, indicating higher SCr and BUN levels and more severe kidney histology compared with Sirt1-intact mice.

It is well-documented that Smad3 phosphorylation is a key signaling mechanism underlying fibrogenesis in response to fibrogenic mediators, such as TGF-β, angiotensin II, and advanced glycation end products [Roberts et al., 2006; Wang et al., 2006; Chung et al., 2010]. Several pieces of evidence from our study suggest that Smad3 acetylation is also an important signaling pathway causing ECM production: (1) 5/6 nephrectomy in rodents or TGF-β1 treatment in cultured cells significantly increases Smad3 acetylation levels; and (2) RSV significantly reduced the Smad3 acetylation levels in the remnant kidney of 5/6 nephrectomized rodents or in cultured cells following TGF-β1 treatment. Knocking down Sirt1 in cultured cells increased acetylation levels of Smad3 and attenuated the effect of RSV on acetylation of Smad3. Our study also showed increased levels of Smad3 phosphorylation in the remnant kidney following 5/6 nephrectomy and in cultured cells following TGF-β1 treatment, consistent with previous findings in the literature [Vindevoghel et al., 1998; Chen et al., 1999]. RSV treatment did not alter the phosphorylation of Smad3.

The acetylation/deacetylation of lysine residues on nuclear proteins has been demonstrated to regulate multiple functions, such as transcriptional activity, DNA binding, protein binding, protein stability, and translocation [Thevenet et al., 2004; Wilson et al., 2010]. Recently, Sirt1-mediated deacetylation of some nuclear proteins, such as p53 [Vaziri et al., 2001; Kume et al., 2006; Yuan et al., 2011], FOXO [Brunet et al., 2004; Hariharan et al., 2010], Smad7 [Kume et al., 2007], and Ku70 [Anekonda and Adamus, 2008], has been reported to regulate cell survival. This study demonstrated the binding of Sirt1 with Samd3 in kidney tissues, as well as in cultured MMCs, and this binding was associated with reduced acetylation levels of Smad3. These results suggest that Sirt1 directly interacts with Smad3, resulting in the deacetylation of Smad3. This study suggests that Smad3 is another transcription factor that can be regulated by Sirt1. The site(s) of acetylation that is regulated by Sirt1 and the detailed mechanism by which acetylation modifies the transcription activity of Smad remain to be explored.

In summary, our findings support that RSV treatment significantly attenuates renal damage in subtotal nephrectomized rats. The renal

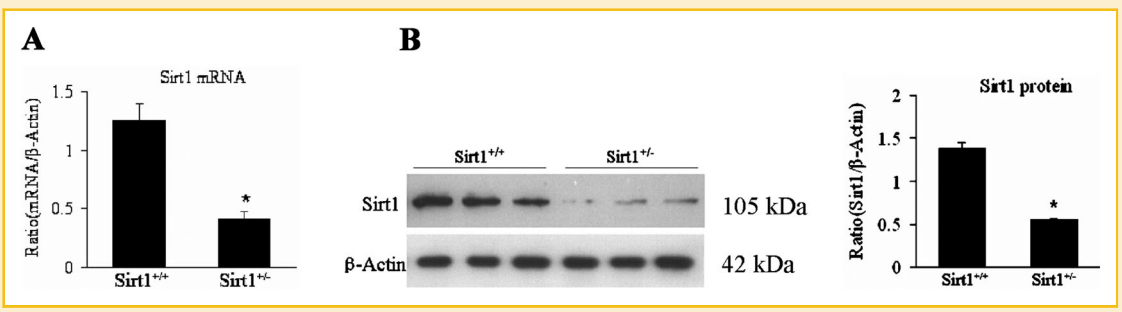

Fig. 7. Reduced Sirt1 expression in the kidney of heterozygous Sirt1-knockout mice. A: Relative Sirt1 mRNA expression level in the entire kidney of wild-type ($Sirt1^{+/+}$) mice and heterozygous Sirt1-knockout ($Sirt1^{+/-}$) mice was examined by real-time PCR. B: Sirt1 protein expression level in the entire kidney of $Sirt1^{+/+}$ and $Sirt1^{+/-}$ mice was examined by Western blot. Data are means ± SE for three independent experiments. $^{*}P < 0.01$ versus the kidney of $Sirt1^{+/+}$ mice.

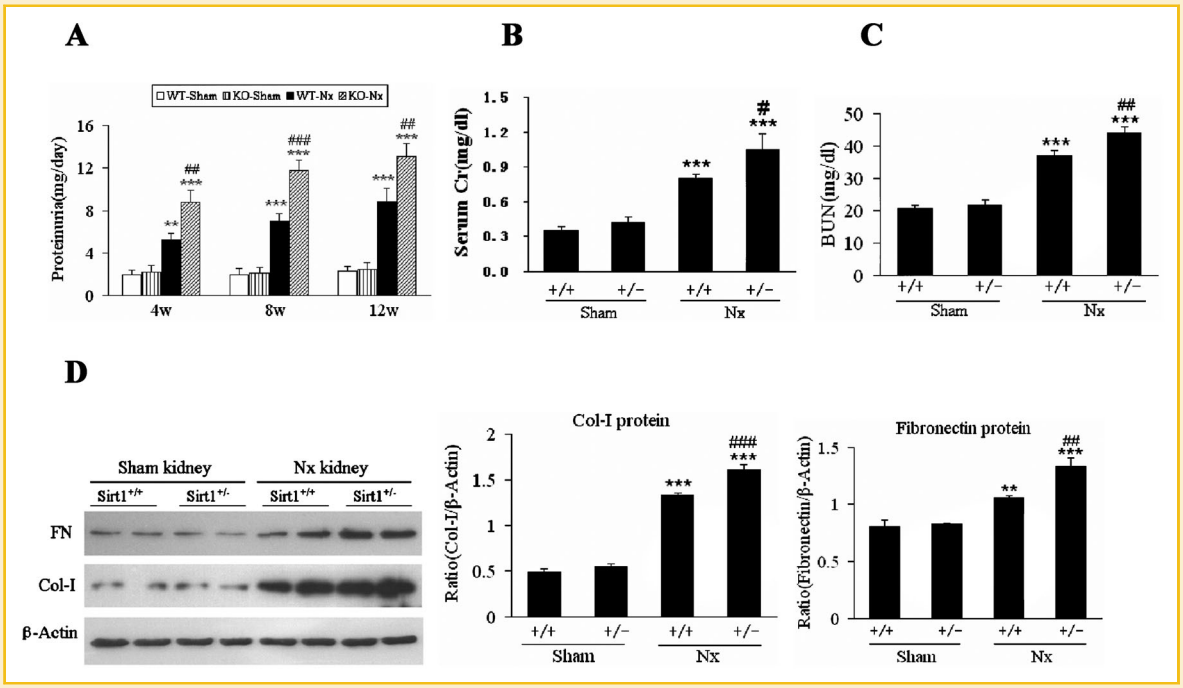

Fig. 8. Sirt1 deficiency aggravates renal function and histological changes in a mouse model of 5/6Nx. Changes in (A) proteinuria, (B) serum creatinine, and (C) BUN in sham-operated or 5/6 nephrectomized Sirt1$^{+/+}$ and Sirt1$^{+/-}$ mice are shown. (D) Levels of fibronectin and collagen I protein expression in the entire kidney of Sirt1$^{+/+}$ and Sirt1$^{+/-}$ mice 12 weeks after 5/6Nx were assessed by Western blot. Data are means ± SE; $^{**}P < 0.01$, $^{***}P < 0.001$ versus WT-Sham; $^{\#}P < 0.05$, $^{\#\#}P < 0.01$, $^{\#\#\#}P < 0.001$ versus WTNx.

protective effect is associated with Sirt1 activation and reduced Smad3 acetylation and TGF-β signaling. These findings indicate that Sirt1 may be a potential therapeutic target for CKD through its effect on renal fibrosis.

ACKNOWLEDGMENTS

This study was supported by grants from the National Natural Science Foundation (no.81130075), Major State Basic Research Development Program of China (973 program) 2012CB517700, 973 program (no.2011CB944000), and 985 Project of China 985III-YFX0302 (to Chuan-Ming Hao), and Science and technology Foundation of Nantong (no.BK2013006) (to Xinzhong Huang).

REFERENCES

Alcendor RR, Gao S, Zhai P, Zablocki D, Holle E, Yu X, Tian B, Wagner T, Vatner SF, Sadoshima J. 2007. Sirt1 regulates aging and resistance to oxidative stress in the heart. Circ Res 100:1512–1521.

Amat R, Planavila A, Chen SL, Iglesias R, Giralt M, Villarroya F. 2009. SIRT1 controls the transcription of the peroxisome proliferator-activated receptor-gamma Co-activator-1alpha (PGC-1alpha) gene in skeletal muscle through the PGC-1alpha autoregulatory loop and interaction with MyoD. J Biol Chem 284:21872–21880.

Anekonda TS, Adamus G. 2008. Resveratrol prevents antibody-induced apoptotic death of retinal cells through upregulation of Sirt1 and Ku70. BMC Res Notes 1:122.

Aubin MC, Lajoie C, Clement R, Gosselin H, Calderone A, Perrault LP. 2008. Female rats fed a high-fat diet were associated with vascular dysfunction and cardiac fibrosis in the absence of overt obesity and hyperlipidemia: Therapeutic potential of resveratrol. J Pharmacol Exp Ther 325:961–968.

Badid C, Vincent M, McGregor B, Melin M, Hadj-Aissa A, Veysseyre C, Hartmann DJ, Desmouliere A, Laville M. 2000. Mycophenolate mofetil reduces myofibroblast infiltration and collagen III deposition in rat remnant kidney. Kidney Int 58:51–61.

Border WA, Noble NA. 1997. TGF-beta in kidney fibrosis: A target for gene therapy. Kidney Int 51:1388–1396.

Bottinger EP, Bitzer M. 2002. TGF-beta signaling in renal disease. J Am Soc Nephrol 13:2600–2610.

Brunet A, Sweeney LB, Sturgill JF, Chua KF, Greer PL, Lin Y, Tran H, Ross SE, Mostoslavsky R, Cohen HY, Hu LS, Cheng HL, Jedrychowski MP, Gygi SP, Sinclair DA, Alt FW, Greenberg ME. 2004. Stress-dependent regulation of FOXO transcription factors by the SIRT1 deacetylase. Science 303:2011–2015.

Chen J, Boyle S, Zhao M, Su W, Takahashi K, Davis L, Decaestecker M, Takahashi T, Breyer MD, Hao CM. 2006. Differential expression of the intermediate filament protein nestin during renal development and its localization in adult podocytes. J Am Soc Nephrol 17:1283–1291.

Chen J, Zhao M, Rao R, Inoue H, Hao CM. 2005. C/EBP{beta} and its binding element are required for NF{kappa}B-induced COX2 expression following hypertonic stress. J Biol Chem 280:16354–16359.

Chen SJ, Yuan W, Mori Y, Levenson A, Trojanowska M, Varga J. 1999. Stimulation of type I collagen transcription in human skin fibroblasts by TGF-beta: Involvement of Smad 3. J Invest Dermatol 112:49–57.

Cheng HL, Mostoslavsky R, Saito S, Manis JP, Gu Y, Patel P, Bronson R, Appella E, Alt FW, Chua KF. 2003. Developmental defects and p53 hyperacetylation in Sir2 homolog (SIRT1)-deficient mice. Proc Natl Acad Sci USA 100:10794–10799.

Chung AC, Zhang H, Kong YZ, Tan JJ, Huang XR, Kopp JB, Lan HY. 2010. Advanced glycation end-products induce tubular CTGF via TGF-beta-independent Smad3 signaling. J Am Soc Nephrol 21:249–260.

Costa Cdos S, Hammes TO, Rohden F, Margis R, Bortolotto JW, Padoin AV, Mottin CC, Guaragna RM. 2010. SIRT1 transcription is decreased in visceral adipose tissue of morbidly obese patients with severe hepatic steatosis. Obes Surg 20:633–639.

Das C, Lucia MS, Hansen KC, Tyler JK. 2009. CBP/p300-mediated acetylation of histone H3 on lysine 56. Nature 459:113–117.

Dennler S, Itoh S, Vivien D, ten Dijke P, Huet S, Gauthier JM. 1998. Direct binding of Smad3 and Smad4 to critical TGF beta-inducible elements in the promoter of human plasminogen activator inhibitor-type 1 gene. EMBO J 17:3091–3100.

Flanders KC. 2004. Smad3 as a mediator of the fibrotic response. Int J Exp Pathol 85:47–64.

Hao CM, Haase VH. 2010. Sirtuins and their relevance to the kidney. J Am Soc Nephrol 21:1620–1627.

Hariharan N, Maejima Y, Nakae J, Paik J, Depinho RA, Sadoshima J. 2010. Deacetylation of FoxO by Sirt1 plays an essential role in mediating starvation-induced autophagy in cardiac myocytes. Circ Res 107:1470–1482.

Hashem MA, Jun KY, Lee E, Lim S, Choo HY, Kwon Y. 2008. A rapid and sensitive screening system for human type I collagen with the aim of discovering potent anti-aging or anti-fibrotic compounds. Mol Cells 26:625–630.

He W, Wang Y, Zhang MZ, You L, Davis LS, Fan H, Yang HC, Fogo AB, Zent R, Harris RC, Breyer MD, Hao CM. 2010. Sirt1 activation protects the mouse renal medulla from oxidative injury. J Clin Invest 120:1056–1068.

Inanaga K, Ichiki T, Matsuura H, Miyazaki R, Hashimoto T, Takeda K, Sunagawa K. 2009. Resveratrol attenuates angiotensin II-induced interleukin-6 expression and perivascular fibrosis. Hypertens Res 32:466–471.

Inoue Y, Itoh Y, Abe K, Okamoto T, Daitoku H, Fukamizu A, Onozaki K, Hayashi H. 2007. Smad3 is acetylated by p300/CBP to regulate its transactivation activity. Oncogene 26:500–508.

Kitada M, Takeda A, Nagai T, Ito H, Kanasaki K, Koya D. 2011. Dietary restriction ameliorates diabetic nephropathy through anti-inflammatory effects and regulation of the autophagy via restoration of Sirt1 in diabetic Wistar fatty (fa/fa) rats: A model of type 2 diabetes. Exp Diabetes Res 2011:908185.

Kume S, Haneda M, Kanasaki K, Sugimoto T, Araki S, Isono M, Isshiki K, Uzu T, Kashiwagi A, Koya D. 2006. Silent information regulator 2 (SIRT1) attenuates oxidative stress-induced mesangial cell apoptosis via p53 deacetylation. Free Radic Biol Med 40:2175–2182.

Kume S, Haneda M, Kanasaki K, Sugimoto T, Araki S, Isshiki K, Isono M, Uzu T, Guarente L, Kashiwagi A, Koya D. 2007. SIRT1 inhibits transforming growth factor beta-induced apoptosis in glomerular mesangial cells via Smad7 deacetylation. J Biol Chem 282:151–158.

Li J, Qu X, Ricardo SD, Bertram JF, Nikolic-Paterson DJ. 2010. Resveratrol inhibits renal fibrosis in the obstructed kidney: Potential role in deacetylation of Smad3. Am J Pathol 177:1065–1071.

Liu Y. 2006. Renal fibrosis: New insights into the pathogenesis and therapeutics. Kidney Int 69:213–217.

Meng XM, Huang XR, Chung AC, Qin W, Shao X, Igarashi P, Ju W, Bottinger EP, Lan HY. 2010. Smad2 protects against TGF-beta/Smad3-mediated renal fibrosis. J Am Soc Nephrol 21:1477–1487.

Park SJ, Ahmad F, Philp A, Baar K, Williams T, Luo H, Ke H, Rehmann H, Taussig R, Brown AL, Kim MK, Beaven MA, Burgin AB, Manganiello V, Chung JH. 2012. Resveratrol ameliorates aging-related metabolic phenotypes by inhibiting cAMP phosphodiesterases. Cell 148:421–433.

Planavila A, Iglesias R, Giralt M, Villarroya F. 2011. Sirt1 acts in association with PPARalpha to protect the heart from hypertrophy, metabolic dysregulation, and inflammation. Cardiovasc Res 90:276–284.

Queen BL, Tollefsbol TO. 2010. Polyphenols and aging. Curr Aging Sci 3:34–42.

Rasouri S, Lagouge M, Auwerx J. 2007. SIRT1/PGC-1: A neuroprotective axis?. Med Sci (Paris) 23:840–844.

Roberts AB, Russo A, Felici A, Flanders KC. 2003. Smad3: A key player in pathogenetic mechanisms dependent on TGF-beta. Ann N Y Acad Sci 995:1–10.

Roberts AB, Tian F, Byfield SD, Stuelten C, Ooshima A, Saika S, Flanders KC. 2006. Smad3 is key to TGF-beta-mediated epithelial-to-mesenchymal transition, fibrosis, tumor suppression and metastasis. Cytokine Growth Factor Rev 17:19–27.

Salminen A, Kaarniranta K. 2009. NF-kappaB signaling in the aging process. J Clin Immunol 29:397–405.

Schnaper HW, Hayashida T, Poncelet AC. 2002. It's a Smad world: Regulation of TGF-beta signaling in the kidney. J Am Soc Nephrol 13:1126–1128.

Shi Y, Massague J. 2003. Mechanisms of TGF-beta signaling from cell membrane to the nucleus. Cell 113:685–700.

Simonsson M, Kanduri M, Gronroos E, Heldin CH, Ericsson J. 2006. The DNA binding activities of Smad2 and Smad3 are regulated by coactivator-mediated acetylation. J Biol Chem 281:39870–39880.

Tanno M, Kuno A, Yano T, Miura T, Hisahara S, Ishikawa S, Shimamoto K, Horio Y. 2010. Induction of manganese superoxide dismutase by nuclear translocation and activation of SIRT1 promotes cell survival in chronic heart failure. J Biol Chem 285:8375–8382.

Thevenet L, Mejean C, Moniot B, Bonneaud N, Galeotti N, Aldrian-Herrada G, Poulat F, Berta P, Benkirane M, Boizet-Bonhoure B. 2004. Regulation of human SRY subcellular distribution by its acetylation/deacetylation. EMBO J 23:3336–3345.

Vaziri H, Dessain SK, Ng Eaton E, Imai SI, Frye RA, Pandita TK, Guarente L, Weinberg RA. 2001. hSIR2(SIRT1) functions as an NAD-dependent p53 deacetylase. Cell 107:149–159.

Vindevoghel L, Lechleider RJ, Kon A, de Caestecker MP, Uitto J, Roberts AB, Mauviel A. 1998. SMAD3/4-dependent transcriptional activation of the human type VII collagen gene (COL7A1) promoter by transforming growth factor beta. Proc Natl Acad Sci USA 95:14769–14774.

Wang W, Huang XR, Canlas E, Oka K, Truong LD, Deng C, Bhowmick NA, Ju W, Bottinger EP, Lan HY. 2006. Essential role of Smad3 in angiotensin II-induced vascular fibrosis. Circ Res 98:1032–1039.

Wang W, Koka V, Lan HY. 2005. Transforming growth factor-beta and Smad signalling in kidney diseases. Nephrology 10:48–56.

Wilson BJ, Tremblay AM, Deblois G, Sylvain-Drolet G, Giguere V. 2010. An acetylation switch modulates the transcriptional activity of estrogen-related receptor alpha. Mol Endocrinol 24:1349–1358.

Yuan F, Xie Q, Wu J, Bai Y, Mao B, Dong Y, Bi W, Ji G, Tao W, Wang Y, Yuan Z. 2011. MST1 promotes apoptosis through regulating Sirt1-dependent p53 deacetylation. J Biol Chem 286:6940–6945.

Zhang Q, Qiu J, Li H, Lu Y, Wang X, Yang J, Wang S, Zhang L, Gu Y, Hao CM, Chen J. 2011. Cyclooxygenase 2 promotes parathyroid hyperplasia in ESRD. J Am Soc Nephrol 22:664–672.

SUPPORTING INFORMATION

Additional supporting information may be found in the online version of this article at the publisher's web-site.